

## Docking studies on novel bisphenylbenzimidazoles (BPBIs) as non-nucleoside inhibitors of HIV-1 reverse transcriptase

Madhu Yadav, Anuradha Singh & Ramendra K Singh\*

Bioorganic Research Laboratory, Department of Chemistry  
University of Allahabad, Allahabad 211 002, India  
E-mail: rksinghsrk@gmail.com

Received 11 March 2016; accepted (revised) 20 February 2017

The low toxicity of non-nucleoside reverse transcriptase inhibitors (NNRTIs) in comparison to nucleoside reverse transcriptase inhibitors (NRTIs) has triggered the idea of preparing better and safer second generation NNRTIs. In this direction, a series of *N*-1 and *C*-2 Bisphenylbenzimidazoles (BPBIs) have been designed *in silico* as possible NNRTIs. On the basis of Lipinski's rule of five, compounds having drug like character have been docked into the active site of human immunodeficiency virus type 1 reverse transcriptase (HIV-1 RT) enzyme (PDB: ID 1HNV) using the software Discovery Studio 2.5. Analysis of the docking results reveal that all molecules form hydrogen bonds with amino acids Lys101, Lys103, Tyr181, Tyr318 and exhibit  $\pi$ -stacking interactions with Tyr181, Tyr188, Phe227 and Trp229 present in the non-nucleoside inhibitor binding pocket (NNIBP). The designed ligands have adopted butterfly conformation inside the NNIBP and form more stable complexes (total interaction energy found in the range of (-) 45.05 – (-) 62.54 kcal/mol) with HIV-1 RT in comparison to TIBO and nevirapine (NVP) (-) 47.70 and (-) 45.99 Kcal/mol, respectively, and thus, lower EC<sub>50</sub> values are predicted for BPBIs. The results provide insight into predictive and diagnostic aspects for better activity of this class of HIV-1 RT inhibitors.

**Keywords:** HIV-1 RT, NNRTI, NNIBP, BPBI, stacking interaction

The enzyme human immunodeficiency virus type 1 reverse transcriptase (HIV-1 RT) is an excellent target for drug design since it is essential for HIV replication and has no effect on normal cell replication<sup>1</sup>. Currently, two classes of antiretroviral drugs are being used to inhibit the reverse transcriptase (RT) reaction: the nucleoside reverse transcriptase inhibitors (NRTIs) and the non-nucleoside reverse transcriptase inhibitors (NNRTIs). NRTIs are the structural analogs of the natural substrates for the enzyme<sup>2</sup>. The NNRTIs are characterized by a high chemical diversity and inhibit RT through interaction within a hydrophobic pocket located at a distance of around 10 Å from its catalytic site. NNRTIs are especially attractive drug candidates because neither they function as chain terminators nor bind at the catalytic site, thus making them less likely to interfere with the normal function of other DNA polymerases and therefore, less toxic than nucleoside inhibitors, such as azidothymidine (AZT). This specificity results in high selectivity index (ratio of *in vitro* cytotoxicity over antiviral activity) for this class of compounds<sup>3,4</sup>.

Activity of an NNRTI is due to its hydrophobic property – a driving force for binding of an NNRTI

into the allosteric pocket of RT. For NNRTI binding, a planar  $\pi$ -electron system and the ability of the system to adopt a conformation designated as the “butterfly-like-orientation” must be present<sup>5</sup>. One wing of the butterfly is made up of  $\pi$ -electron rich moiety (phenyl or allyl substituents), which interacts through  $\pi$ - $\pi$  interaction with hydrophobic pocket formed mainly by the side chains of aromatic amino acids (Tyr181, Tyr188, Phe227, Trp229, Tyr318). The wing II is normally represented by a heteroaromatic ring bearing on one side a functional group capable of donating or accepting hydrogen bonds with main chain of Lys101 and Lys103, and the butterfly body, a hydrophobic portion fulfills a small pocket formed mainly by side chains of Lys103, Val106, and Val179. In such structures, the wing I aromatic ring has extensive hydrophobic interactions whereas wing II has relatively fewer interactions with the surrounding amino acid residues in this pocket. For NNRTI binding with RT pocket,  $\pi$ -stacking and van der Waals interactions are very important<sup>6,7</sup>.

NNRTIs, such as tetrahydro-imidazo[4,5,1jk][1,4]-benzodiazepin-2(1*H*)one (TIBO), have shown significant activity for RT inhibition. The first

benzimidazole derivatives reported as potential anti-HIV-1 agents were the 1-aryl-1*H*,3*H*-thiazolo[3,4-*a*]benzimidazoles (TBZs), which proved to be highly active as NNRTIs<sup>8</sup>. Specifically, TBZ 1-(2,6-difluorophenyl)-3*H*-[1,3]thiazolo[3,4-*a*]benzimidazole has been shown clearly to be the most potent inhibitor, and is considered as a lead compound for 2-aryl-substituted benzimidazole derivatives<sup>9</sup>. Substituents on the benzimidazole ring can significantly improve binding of BPBIs to the NNRTI binding pocket residues. Thus, the biological activity of NNRTIs depends on suitable spatial location of lipophilic and electron-rich groups in the hydrophobic pocket of the enzyme<sup>10-13</sup>. On the basis of extensive literature survey and keeping the above facts in mind, we have designed several derivatives of bisphenyl-benzimidazole (BPBI), structurally similar to TIBO, TBZ and nevirapine (Figure 1), docked them with HIV-1 RT and performed computational studies using TIBO and nevirapine as standards.

## Materials and Method

### *In silico* design of compounds

We have analysed some physically significant descriptors and pharmaceutically relevant properties, like molecular weight, H-bond donors, H-bond acceptors, log P (octanol/water), of BPBIs on the basis of Lipinski's rule of five<sup>14</sup> using Molinspiration and ChemDraw softwares.

All these filtered molecules were further subjected to docking. The structure retrieved from the Protein Data Bank ([www.rcsb.org](http://www.rcsb.org)) with entry code 1HNV, has been utilized for modelling studies taking BPBIs, 8-Cl TIBO and nevirapine as ligands<sup>15</sup>.

### Receptor setup

The target protein [PDB ID: 1HNV] was taken, the ligand TIBO extracted, the missing hydrogens were added, and their positions optimized using the all-atom CHARMM (version-c32b1) forcefield<sup>16,17</sup> and

the Adopted Basis set Newton Raphson (ABNR) method available in DS 2.5 protocol (Discovery Studio 2.5, 2011) until the root mean square (r.m.s.) gradient was less than 0.05 kcal mol<sup>-1</sup> Å<sup>-1</sup>. Minimization was performed to relax these newly added hydrogen atoms by fixing all other non-hydrogen atoms. The minimized structure of the protein was used in docking simulations. The minimized protein was defined as the 'receptor' using the binding site module of DS 2.5. The binding site was defined from the volume of ligand method, which was modified to accommodate all important interacting residues in the active site of HIV-1 RT. The Input Site Sphere was defined over the binding site, with a radius of 5 Å from the centre of the binding site. Input Site Sphere parameters specify a sphere around the center of the binding site, where the docking is to be performed. The center of the "Input Site Sphere" is used for the initial ligand placement. The protein, thus characterized, was taken as the target receptor for the docking procedure. The resulting 3-D structure is saved in mol files.

### Ligand setup

In order to propose new inhibitors, build-and-edit module of DS 2.5 is used. A series of desired BPBIs (Table I), having substitution at *N*-1 and *C*-2, was built, all-atom CHARMM forcefield (version c32b1) was assigned and then minimized using the adopted basis Newton-Raphson (ABNR) method as described above. A conformational search of BPBIs was carried out using a simulated annealing molecular dynamics (MD) approach. The ligand was heated to a temperature of 700 K and then annealed to 200 K to maintain thermal equilibrium of the molecule. Thirty such cycles were carried out. The conformation obtained at the end of each cycle was further subjected to local energy minimization, using Smart Minimizer method (steepest descent followed by

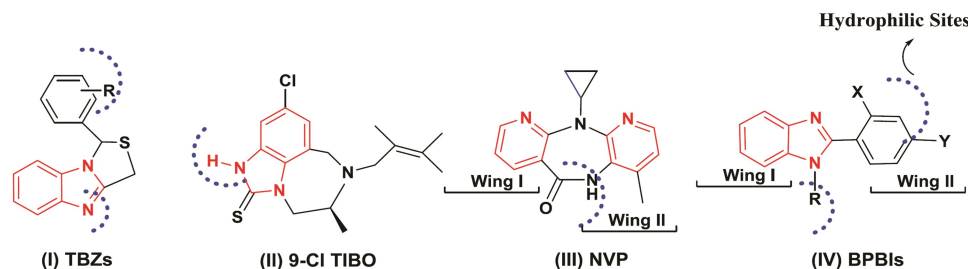


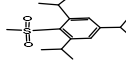
Figure 1 — Structural similarities between reported NNRTIs (I-III) and the designed BisPhenylBenzImidazoles (BPBIs) (IV) showing hydrophobic parts (red) and hydrophilic parts (blue dotted circles)

Table I — Structure and Physicochemical descriptors of BPBIs

Ligand	-X	-Y	-R	MW <sup>a</sup>	H-A <sup>b</sup>	H-D <sup>c</sup>	LogP <sup>d</sup>	TPSA <sup>e</sup>	MV <sup>f</sup>	Violations
1	-NO <sub>2</sub>	-H		449.49	8	0	5.56	91.35	379.90	1
2	-H	-NO <sub>2</sub>		449.49	8	0	5.61	91.35	379.90	1
3	-NO <sub>2</sub>	-H		427.40	5	0	6.43	63.65	334.56	1
4	-H	-NO <sub>2</sub>		427.40	5	0	6.48	63.65	334.56	1
5	-NO <sub>2</sub>	-H		359.41	5	0	5.59	63.65	303.66	1
6	-H	-NO <sub>2</sub>		359.41	5	0	5.59	63.65	303.26	1
7	-NO <sub>2</sub>	-H		409.56	5	0	8.38	63.65	382.83	1
8	-H	-NO <sub>2</sub>		409.56	5	0	8.38	63.65	382.83	1
9	-H	-NO <sub>2</sub>		428.40	6	0	5.60	76.54	330.40	1
10	-NO <sub>2</sub>	-H		428.40	6	0	5.60	76.54	330.40	1
11	-H	-NH <sub>2</sub>		288.35	4	2	3.28	48.78	265.52	0
12	-H	-NO <sub>2</sub>		318.34	6	0	4.17	68.58	277.57	0
13	-NO <sub>2</sub>	-H		318.34	6	0	4.12	68.58	277.57	0
14	-H	-OH		289.34	4	1	3.73	42.99	262.25	0
15	-NO <sub>2</sub>	-H		413.84	7	0	5.11	97.79	320.37	1
16	-H	-NO <sub>2</sub>		413.84	7	0	5.11	97.79	320.37	1
17	-NO <sub>2</sub>	-H		424.39	10	0	4.39	143.62	330.16	0
18	-H	-NO <sub>2</sub>		424.39	10	0	4.39	143.62	330.16	0
19	-NO <sub>2</sub>	-H		371.30	7	0	6.50	97.79	266.72	1
20	-H	-NO <sub>2</sub>		371.30	7	0	6.50	97.79	266.72	1
21	-NO <sub>2</sub>	-H		505.64	7	0	7.88	97.79	456.68	2

Contd —

Table I — Structure and Physicochemical descriptors of BPBIs—Contd

Ligand	-X	-Y	-R	MW <sup>a</sup>	H-A <sup>b</sup>	H-D <sup>c</sup>	LogP <sup>d</sup>	TPSA <sup>e</sup>	MV <sup>f</sup>	Violations
<b>22</b>	-H	-NO <sub>2</sub>		505.64	7	0	7.88	97.79	456.68	2
<b>TIBO</b>				321.877	3	1	3.737	23.963	286.06	0
<b>NVP</b>				266.30	5	1	1.38	63.58	242.56	0

<sup>a</sup>Molecular weight, <sup>b</sup>number of H bond acceptors, <sup>c</sup>number of H bond donors, <sup>d</sup>Octanol-water partition coefficient, <sup>e</sup>Total polar surface area, <sup>f</sup>Molecular volume

conjugate gradient) with 2000 steps and r.m.s. gradient of 0.001 kcal mol<sup>-1</sup> Å<sup>-1</sup> with the help of ABNR method as described above. The 30 energy-minimized structures were then superimposed and the lowest energy conformation occurring in the major cluster was taken to be the most probable conformation.

### Docking and scoring

Binding mode of BPBIs can be explored by using the RT-TIBO complex for Ligand Fit docking protocol<sup>18</sup>. Ligand Fit algorithm performed a shape comparison filter with a Monte Carlo conformational search (bond lengths and bond angles were fixed, only the rotatable bonds were allowed to rotate freely) to generate docked poses parallel to the shape of the binding site. Dreiding forcefield, a grid-based calculated interaction energy, is used to refine these poses by rigid body minimization<sup>19</sup>. The receptor protein was fixed during docking. The docked poses were further minimized by using all-atom CHARMM forcefield and smart minimizer algorithm until the r.m.s gradient for potential energy was less than 0.001 kcal mol<sup>-1</sup> Å<sup>-1</sup> and evaluated with a set of scoring functions. The atoms of ligand and the side chains of the residues of the receptor within 5 Å from the centre of the binding site were kept flexible during minimization. The LUDI III score was used to score the refined poses<sup>20-22</sup>. The ligand pose which corresponded to the highest LUDI III score was taken as the best docked pose<sup>23</sup>.

### Validation of the docking methodology

Docking was first tested on known inhibitors—nevirapine and TIBO, which were docked in the allosteric binding site of HIV-1 RT, after extracting the ligand from the crystal structure.

The root mean square deviation (RMSD) of the best docked poses of the molecules reported herein was less than 2 Å, which is supposed to be an appropriate condition for developing NNRTIs. Two structures overlap very well with positional RMSD of 1.2. The docked pose having the highest LUDI III score gave the least RMSD with respect to the crystal conformation for both the ligands. Thus, LUDI III is an empirical scoring function, which is used to predict the binding affinity of the ligands when complexed with the protein.

### Results and Discussion

Drug-like properties of the mapped compounds were assessed through the Lipinski's rule of five in order to exclude unnecessary molecules. The mapped compounds that satisfied the rules, *i.e.*, (i) less than 5 hydrogen bond donors, (ii) not more than 10 hydrogen bond acceptors, (iii) molecular weight not greater than 500, and (iv) logP value less than 5, were selected as drug-like compounds. Molecules violating more than one of these rules may have problems with bioavailability and hence rejected. In the present study (Table I) **20** out of **22** ligands, showed the allowed values for the properties analysed and exhibited drug-like characteristics based on Lipinski's rule of five. So, the molecules selected showed high potential to cross the cell membrane. The analogues **21** and **22**, did not show drug-like characteristics. It may be due to their large size (big molecular volume) and molecular weight.

Ligand pose geometry docked into a target receptor structure was rigorously analyzed through scoring functions, such as PLP1, PLP2, PMF, Lig\_Internal\_Energy, binding energy, dock score and ultimately Ludi3. All the scoring data for the title

hybrid BPBIs along with reference nevirapine and TIBO are presented in Table II. Piecewise Linear Potential (PLP) scores explain the protein ligand binding affinities and reported as negative values. Higher PLP score indicated stronger receptor-ligand interaction. PLP1 and PLP2 are two available versions of the PLP function<sup>24</sup>. Each non-hydrogen ligand or non-hydrogen receptor atom is assigned a PLP atom type in the PLP1 function. In PLP2 function, PLP atom types remain the same as in PLP1. In addition, an atomic radius is assigned to each atom except for hydrogen. Majority of title BPBIs showed comparable PLP scores to the reference ligands. The PMF scoring functions were found to correlate well with protein-ligand binding free energies<sup>25</sup>. In a comparison test, it was found that all title compounds showed significant PMF scores with reference to the standard ligand. The internal ligand energy consists of a van der Waals (vdW) term and an optional electrostatic term. The non-bonded vdW energy is computed using a standard 9-6 (unsoftened) potential

using force field parameters consistent with the force field employed. Efficient ligand is classified with high negative ligand internal energy. Table II illustrated that ligand internal energy (kcal/mol) of compounds **2** (-5.29), **5** (-5.04), **6** (-5.78), **17** (-5.40), **18** (-5.26) and **19** (-5.38) was similar to that of reference nevirapine (-5.35), whereas in the case of compounds **4** (-0.22), **13** (-0.12), **15** (-0.83) and **13** (-0.43), the ligand internal energy was similar to that of reference TIBO (-0.42). All BPBIs have similar mode of binding and significant binding affinity towards NNIBP receptor domain as that of the reference ligand as reflected from Dock Score function, which evaluates and prioritizes candidate ligand poses. The reference ligand nevirapine exhibited dock score of 50.85 and BPBIs showed dock score ranging from 42.88 to 57.62. The binding free energies for each BPBI derivative was predicted using the Ludi scoring function. The molecules **1**, **2**, **3**, **7**, **8**, **9**, **10** and **17** have much lower interaction energies than the nevirapine and TIBO. So these

Table II — Scoring and stability of HIV-1 RT- ligand complexes

Ligand	Docked energy (kcalmol <sup>-1</sup> )			DS <sup>a</sup>	-PLP1 <sup>b</sup>	-PLP2 <sup>b</sup>	-PMF <sup>c</sup>	LIG <sup>d</sup>	Ludi_2 <sup>e</sup>	ΔG <sub>pred</sub> <sup>f</sup>	Ludi_3 <sup>e</sup>	Predicted EC <sub>50</sub> <sup>g</sup>
	van der Waals energy (kcal/mol)	Electrostatic energy (kcal/mol)	Total interaction energy (kcal/mol)									
<b>1</b>	-49.85	-9.09	-58.94	50.19	114.97	106.83	110.74	-2.47	550	-7.80	726	5.50×10 <sup>-2</sup>
<b>2</b>	-57.06	-5.48	-62.54	57.62	113.45	96.86	90.83	-5.29	578	-8.20	742	3.8×10 <sup>-2</sup>
<b>3</b>	-50.98	-5.25	-56.23	56.11	91.84	104.29	91.56	-2.93	477	-6.77	814	7.24×10 <sup>-3</sup>
<b>4</b>	-30.96	-12.96	-43.92	54.93	90.73	104.49	79.27	-0.22	533	-7.56	990	1.2×10 <sup>-4</sup>
<b>5</b>	-44.11	-3.54	-47.64	54.86	88.17	82.76	94.07	-5.04	443	-6.28	604	9.12×10 <sup>-1</sup>
<b>6</b>	-43.75	-2.62	-46.37	52.49	92.65	84.92	100.1	-5.78	460	-6.52	628	5.25×10 <sup>-1</sup>
<b>7</b>	-59.94	-1.89	-61.83	43.56	91.22	81	88.79	-4.29	408	-5.78	655	2.82×10 <sup>-1</sup>
<b>8</b>	-54.69	-3.39	-58.08	42.88	107.15	102.92	76.52	-3.57	494	-7.01	698	1.05×10 <sup>-1</sup>
<b>9</b>	-48.69	-4.23	-52.92	55.41	101.91	102.68	96.87	-2.04	522	-7.40	984	1.45×10 <sup>-4</sup>
<b>10</b>	-47.02	-7.15	-54.16	44.16	89.98	90.83	92.55	-1.32	477	-6.77	856	2.75×10 <sup>-3</sup>
<b>11</b>	-41.83	-3.23	-45.05	46.73	91.43	86.78	71.72	-3.98	406	-5.76	629	5.13×10 <sup>-1</sup>
<b>12</b>	-39.18	-6.77	-45.94	51.14	80.39	72.61	91.37	-4.71	407	-5.78	573	1.86
<b>13</b>	-45.81	-2.37	-48.17	43.94	93.62	78.35	77.11	-0.12	404	-5.73	673	1.86×10 <sup>-1</sup>
<b>14</b>	-38.74	-10.67	-49.40	47.95	82.5	79.24	80.35	-3.96	451	-6.39	660	2.5×10 <sup>-1</sup>
<b>15</b>	-45.15	-10.83	-55.97	48.98	96.39	95.3	116.24	-0.83	415	-5.89	864	2.29×10 <sup>-3</sup>
<b>16</b>	-45.22	-10.76	-55.97	53.32	93.8	89.23	102.24	-3.38	429	-6.08	933	4.68×10 <sup>-4</sup>
<b>17</b>	-48.09	-8.870	-56.96	49.56	94.07	89.25	117.39	-5.40	409	-5.80	869	2.04×10 <sup>-3</sup>
<b>18</b>	-45.22	-10.76	-55.97	51.76	84.14	72.68	108.53	-5.26	388	-5.50	897	1.07×10 <sup>-3</sup>
<b>19</b>	-38.06	-13.37	-51.42	48.47	80.02	79.58	49.50	-5.38	346	-4.91	412	.759
<b>20</b>	-39.11	-13.85	-52.96	44.65	72.91	83.76	51.77	-0.43	335	-4.75	413	.741
<b>21</b>												
<b>22</b>												
<b>TIBO</b>	-43.05	-4.65	-47.70	32.39	80.77	75.4	57.04	-0.42	469	-6.67	516	6.92
<b>NVP</b>	-38.53	-7.46	-45.99	50.85	94.81	90.29	103.2	-5.35	470	-6.65	636	5.12×10 <sup>-1</sup>

<sup>a</sup> Dock score, <sup>b</sup> Piecewise Linear Potential, <sup>c</sup> potential of mean force, <sup>d</sup> Ligand internal energy (kcal/mol), <sup>e</sup> Ludi\_2 and Ludi\_3, empirical scoring functions derived from the Ludi algorithm, <sup>f</sup> Predicted Standard binding free energy (kcal/mol), <sup>g</sup> Predicted 50% effective concentration required to inhibit HIV1 replication (μM)

molecules are more stabilized than the known drugs nevirapine and TIBO and their  $\Delta G$  values are also lower, which reflect their high binding affinity. The binding free energy ( $\Delta G$ ) and Predicted  $EC_{50}$  for each derivative were predicted using the Ludi\_2 and Ludi\_3 scoring functions, respectively<sup>26</sup>.

Visualization was done using PyMol software. Visual inspection of the minimized complexes of BPBIs with HIV-1 RT showed the requisite electronic and hydrophobic interactions between the enzyme and the ligands. BPBIs interacted with residues Lys101, Lys103, Tyr181, Tyr188, His235 and Tyr318 through H-bonds and with residues Lys103, Phe227, Trp229, Tyr181, Tyr188 and Tyr318 through  $\pi$ -interactions, present in the NNIBP, where the aryl and benzimidazole cores acted as wing I and II, respectively. In the case of nevirapine and TIBO, H-bonding was absent. The nevirapine interacted through  $\pi$ - $\pi$  interaction with Tyr318 while TIBO showed  $\pi$ -interaction with Tyr181.

The structure-activity relationships (SAR) data, as shown in Table III, revealed that the aromatic substituents at position *N*-1 and *C*-2 of the benzimidazole core played an important role in the stabilization of these compounds within HIV-1 RT. The initial interactions of BPBIs with HIV-1 RT resulted in reorientation of the residues Tyr181, Tyr188 and Trp229, to fully accommodate the BPBIs as inhibitors. The distance for electronic and hydrophobic interactions in the present studies was observed well below the limit of 6 Å for optimum receptor-ligand recognition as suggested by Gallivan and Dougherty<sup>27</sup> and shown in Table III.

Substituted benzothiamide, aryl/alkyl sulphonyl and pyrrol groups are attached to the active 2-aryl-benzimidazole framework. The compounds **3**, **4**, **9**, **10**, **15** and **16**, having -I groups, have shown high binding affinity with HIV-1 RT, which indicated towards better anti-HIV activity. SAR studies on all BPBIs revealed that *C*-2 position on benzimidazole ring played a crucial role in the stabilization of protein-ligand complex. Compounds containing *o*-nitro phenyl group at *C*-2 position on benzimidazole moiety, are more stabilized than compounds having *p*-nitro phenyl group, except for the compound **6**. The  $\pi$ -stacking interactions between the electron-deficient 4-trifluoromethyl benzothiamide ring system present in ligand **3** and electron-rich Tyr181, Tyr188 and Trp229 residues in the binding site resulted in highly fruitful electronic and hydrophobic interactions between the enzyme and the ligand.

Superimposition of all minimized frames showed that the proposed BPBIs bind to the HIV-1 RT in a common mode since chemically equivalent groups fit in a similar orientation within the NNIBP. In compounds **1**, **2** and **13**, the 2-aryl substituent (2/4-nitrophenyl) is placed towards the inside of NNIBP, and is able to establish a H-bond between the nitro group and the Lys101, Lys103 backbone and Tyr318. The  $\pi$ -stacking interactions do contribute to stabilization of the complex as is evident with compound **7** having only the  $\pi$ - $\pi$  and  $\pi$ -cation interactions. In compounds **11**, **12**, **13** and **14** the pyrrol group interacts through the  $\pi$ -stacking interaction with Tyr181 and Tyr188 and provides high stability to the protein-ligand complex.

In compound **5**, *o*-nitro phenyl at *C*-2 of benzimidazole moiety exhibited  $\pi$ -cation interaction with Phe227 and N-3 of benzimidazole nucleus formed H-bond with Lys101.

Compounds **19** and **20** have lower interaction energy and interacted through H-bond formation between  $-SO_2$  and Lys103, and F atoms of  $-CF_3$  group and Lys101 and Tyr318. Compound **20** also showed  $\pi$ -cation interaction with Tyr181 present in NNIBP. However, they have very poor binding affinity that might have resulted due to lack of  $\pi$  electron system in the form of a phenyl ring.

Compounds **3**, **5**, **7**, **8**, **16**, **17**, **18** having benzimidazole nucleus also participated in  $\pi$ -stacking interaction with Lys103, Tyr181 and Tyr188 amino acid residues.

Docking experiment showed quite different patterns of interaction of these molecules in comparison to TIBO. Compounds **2**, **10**, **13** and **20** formed H-bonds which was absent in TIBO. All designed BPBIs except **19** and **20**, have high Ludi values than TIBO.

In general, examination of HIV-1 RT complexes formed by compounds **3**, **4**, **9** and **10** having  $\pi$ -deficient aromatic rings and compounds **15**, **16**, **17**, **18** having substituted sulfonyl moiety with the amino acid residues Tyr181/Tyr188 on HIV-1 RT, revealed that the molecules under study are associated in a coplanar arrangement of their aromatic rings. This allowed favorable  $\pi$ -stacking interactions, which contributed to stabilization of complexes, just like in nevirapine. This spatial arrangement may also lead to a partial charge transfer between the electron-rich aromatic ring of Tyr181/Tyr188 and the electron deficient phenyl ring of the benzothiamide system. Nevertheless, the predicted  $K_d$  value also indicated that the electron-withdrawing effect, which could enhance the above mentioned  $\pi$ -stacking interactions

Table III — Point of interactions of BPBIs with HIV-1 RT

Ligand	No. of H-B	Amino acid in H-B	D (Å)	D-A	A-A	No. of $\pi$ -B	Amino acid in $\pi$ -B	' $\pi$ - $\pi$ '/' $\pi$ -+' monitor Bond	D (Å)	End1	End2
<b>1</b>	1	Lys101	2.9	N	O17	—	—		—	—	—
<b>2</b>	2	Lys101	3.0	N	N7	—	—		—	—	—
		Tyr318	3.1	OH	O49						
<b>3</b>	1	Lys103	2.9	N	F39	6	Tyr181	Tyr 181 : <b>3</b>	4.5	Tyr181	<b>3</b>
							Tyr188	Tyr 188 : <b>3</b>	3.9	Tyr188	<b>3</b>
							Trp229	Tyr 188 : <b>3</b>	4.0	Tyr188	<b>3</b>
								Tyr 181 - <b>3</b> :N16	5.0	Tyr181	<b>3</b> :N16
								Tyr 188 - <b>3</b> :N16	5.7	Tyr188	<b>3</b> :N16
								Trp229 - <b>3</b> :N16	4.1	Trp229	<b>3</b> :N16
<b>4</b>	2	Lys103	3.0	N OH	F36	3	Tyr188	Tyr 181 : <b>4</b>	4.5	Tyr181	<b>4</b> :N38
		Tyr318	3.0		F35		Trp229	Tyr 181 : <b>4</b>	5.3	Tyr181	
								Trp229 - <b>4</b> :N38	5.6	Trp229	
<b>5</b>	1	Lys 101	3.0	N	N7	1	Phe227	' $\pi$ - +' ( Phe227- <b>5</b> :N36)	4.0	Phe227	<b>5</b> :N36
<b>6</b>	—	—	—	—	—	—	Tyr181	' $\pi$ - +' (Tyr 181 - <b>6</b> :N16)	4.6	Tyr181	<b>6</b> : N16
							Tyr188	' $\pi$ - +' (Tyr 188 - <b>6</b> :N16)	6.8	Tyr188	<b>6</b> : N16
<b>7</b>	—	—	—	—	—	5	Tyr181	' $\pi$ - $\pi$ ' (Tyr 181 - <b>7</b> :N16)	5.8	Tyr181	<b>7</b>
								' $\pi$ - +' (Tyr 181 - <b>7</b> :N16)	4.7	Tyr181	<b>7</b> :N16
							Lys103	' $\pi$ - +' (Lys103 - <b>7</b> :N16)	6.8	Lys103	<b>7</b>
							Trp229	' $\pi$ - +' (Trp229- <b>7</b> :N16)	5.4	Trp229	<b>7</b> :N16
								' $\pi$ - +' (Trp229- <b>7</b> :N16)	4.4	Trp229	<b>7</b> :N16
<b>8</b>	—	—	—	—	—	4	Tyr181	' $\pi$ - $\pi$ ' (Tyr 181 - <b>8</b> )	4.8	Tyr 181	<b>8</b>
								' $\pi$ - $\pi$ ' (Tyr 181 - <b>8</b> )	4.3	Tyr 181	<b>8</b>
							Trp229	' $\pi$ - +' (Trp229- <b>8</b> :C27)	4.3	Trp229	<b>8</b> :C27
								' $\pi$ - +' (Trp229- <b>8</b> : C27)	5.0	Trp229	<b>8</b> :C27
<b>9</b>	1	Lys103	3.1	N	O17	—	Tyr181	' $\pi$ - $\pi$ ' (Tyr 181 - <b>9</b> )	3.8	Tyr 188	<b>9</b>
<b>10</b>	2	Tyr181	3.0	N	O17	—	Tyr188	' $\pi$ - $\pi$ ' (Tyr 188 - <b>10</b> )	4.3	Tyr 188	<b>10</b>
		Tyr318	3.0	OH	F41	—					
<b>11</b>	—	—	—	—	—	—	Tyr188	' $\pi$ - $\pi$ ' (Tyr 181 - <b>11</b> )	4.1	Tyr 181	<b>11</b>
<b>12</b>	—	—	—	—	—	—	Lys103	' $\pi$ - +' (Lys103 - <b>12</b> )	6.4	<b>12</b>	Lys103
<b>13</b>	1	Lys 103	3.1	N	O26	2	Tyr 181	' $\pi$ - $\pi$ ' (Tyr 181 - <b>13</b> )	4.9	Tyr 181	<b>13</b>
							Tyr318	' $\pi$ - +' (Tyr 318 - <b>13</b> :N24)	4.7	Tyr 318	<b>13</b> :N24
<b>14</b>	2	Tyr318	2.9	OH	O36	1	Tyr181	' $\pi$ - $\pi$ ' (Tyr 181 - <b>14</b> )	5.2	Tyr 181	<b>14</b>
		His235	2.5	O	O36	—					
<b>15</b>	—	—	—	—	—	—	Tyr181	' $\pi$ - $\pi$ ' (Tyr 181 - <b>15</b> )	5.6	Tyr 181	<b>15</b>
								' $\pi$ - $\pi$ ' (Tyr 181 - <b>15</b> )	4.5	Tyr 181	<b>15</b>
								' $\pi$ - $\pi$ ' (Tyr 181 - <b>15</b> )	4.3	Tyr 181	<b>15</b>
							Tyr188	' $\pi$ - $\pi$ ' (Tyr 188 - <b>15</b> )	4.5	Tyr 188	<b>15</b>
								' $\pi$ - $\pi$ ' (Tyr 188 - <b>15</b> )	4.9	Tyr 188	<b>15</b>
<b>16</b>	—	—	—	—	—	5	Tyr181	' $\pi$ - $\pi$ ' (Tyr 181 - <b>16</b> )	5.5	Tyr 181	<b>16</b>
							Tyr188	' $\pi$ - $\pi$ ' (Tyr 181 - <b>16</b> )	4.4	Tyr 181	<b>16</b>
								' $\pi$ - $\pi$ ' (Tyr 181 - <b>16</b> )	4.2	Tyr 181	<b>16</b>
								' $\pi$ - $\pi$ ' (Tyr 188 - <b>16</b> )	4.5	Tyr 188	<b>16</b>
								' $\pi$ - $\pi$ ' (Tyr 188 - <b>16</b> )	4.7	Tyr 188	<b>16</b>

Contd—

Table III — Point of interactions of BPBIs with HIV-1 RT—*Contd*

Ligand	No. of H-B	Amino acid in H-B	D (Å)	D-A	A-A	No. of $\pi$ -B	Amino acid in $\pi$ -B	' $\pi$ - $\pi$ '/' $\pi$ -+' monitor	Ligand	No. of H-B	Amino acid in H-B
<b>17</b>	—					6	Tyr181	' $\pi$ - $\pi$ ' (Tyr 181 - <b>17</b> )	4.2	Tyr 181	<b>17</b>
								' $\pi$ -+' (Tyr 181 - <b>17</b> :N37)	3.8	Tyr 181	<b>17</b> :N37
							Tyr188	' $\pi$ - $\pi$ ' (Tyr 188- <b>17</b> )	4.6	Tyr 188	<b>17</b>
								' $\pi$ - $\pi$ ' (Tyr 188- <b>17</b> )	5.6	Tyr 188	<b>17</b>
							Phe227	' $\pi$ -+' (Phe227- <b>17</b> :N23)	4.7	Phe227	
							Trp229	' $\pi$ -+' (Trp229- <b>17</b> :N37)	4.4	Trp229	
<b>18</b>	1	Lys103	2.9	N	O42	6	Tyr188	' $\pi$ - $\pi$ ' (Tyr 188 - <b>18</b> )	4.5	Tyr 188	<b>18</b>
							Tyr181	' $\pi$ - $\pi$ ' (Tyr 181- <b>18</b> )	5.5	Tyr 181	<b>18</b>
								' $\pi$ - $\pi$ ' (Tyr 181- <b>18</b> )	4.4	Tyr 181	<b>18</b>
								' $\pi$ - $\pi$ ' (Tyr 181- <b>18</b> )	4.2	Tyr 181	<b>18</b>
							Phe227	' $\pi$ -+' (Phe227- <b>18</b> :N23)	6.4	Phe227	<b>18</b>
							Tyr318	' $\pi$ -+' (Tyr 318 - <b>18</b> :N23)	4.7	Tyr 318	<b>18</b> :N23
<b>19</b>	1	Lys 103	2.8	N	O17		—	—	—	—	—
<b>20</b>	3	Lys103	3.1	N	F31	1	Tyr181	' $\pi$ -+' (Tyr 181 - <b>20</b> :N20)	4.1	Tyr 181	<b>20</b> :N20
		Lys101	2.8	N	O17						
		Tyr318	3.0	OH	F32						
<b>21</b>							DID NOT DOCK				
<b>22</b>							DID NOT DOCK				
<b>TIBO</b>							Tyr181				
<b>NVP</b>	0	—	—	—	—	2	Tyr181	6.0	Tyr181		
							(' $\pi$ - $\pi$ ')	5.1	Tyr188		
							Tyr188				
							(' $\pi$ - $\pi$ ')				

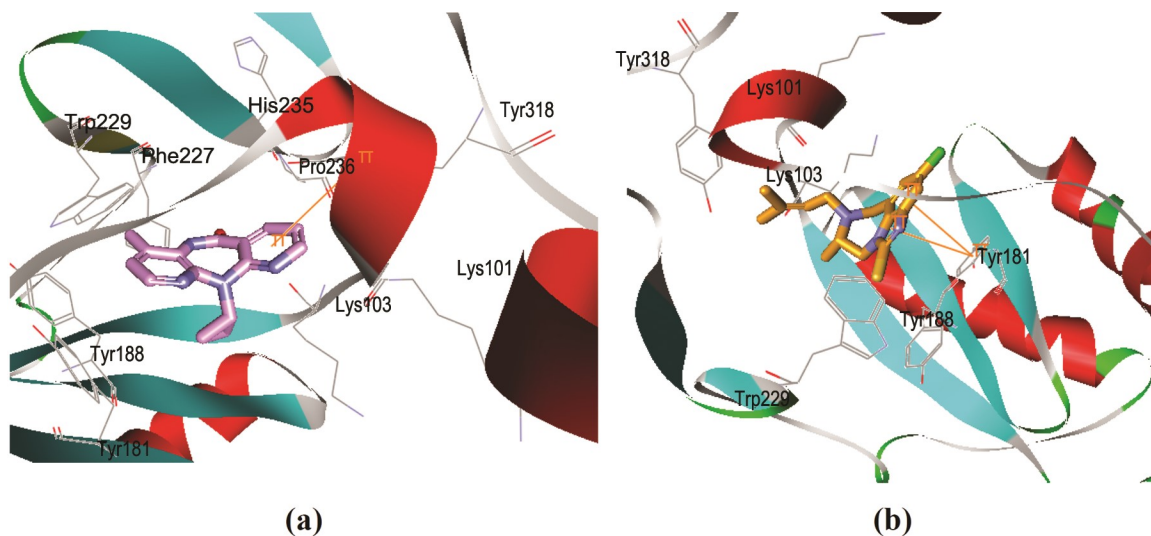


Figure 2 — Interactions of (a) NVP and (b) TIBO into allosteric site of HIV-1 RT

through the phenyl ring of the benzothiamide system, is not enough for strong inhibition of HIV-1 RT. The substitution pattern of this ring, especially at *N*-1 and *C*-2, is very important for the inhibitory activity of these molecules. The results indicated that the ligands as a whole moved into a

more stable position with a much lower docked energy. It can be seen from Figure 2 and Figure 3 that the designed inhibitors occupied a position similar to that as TIBO/ nevirapine.

When the newly introduced BPBIs having higher LUDI III score than TIBO/nevirapine were



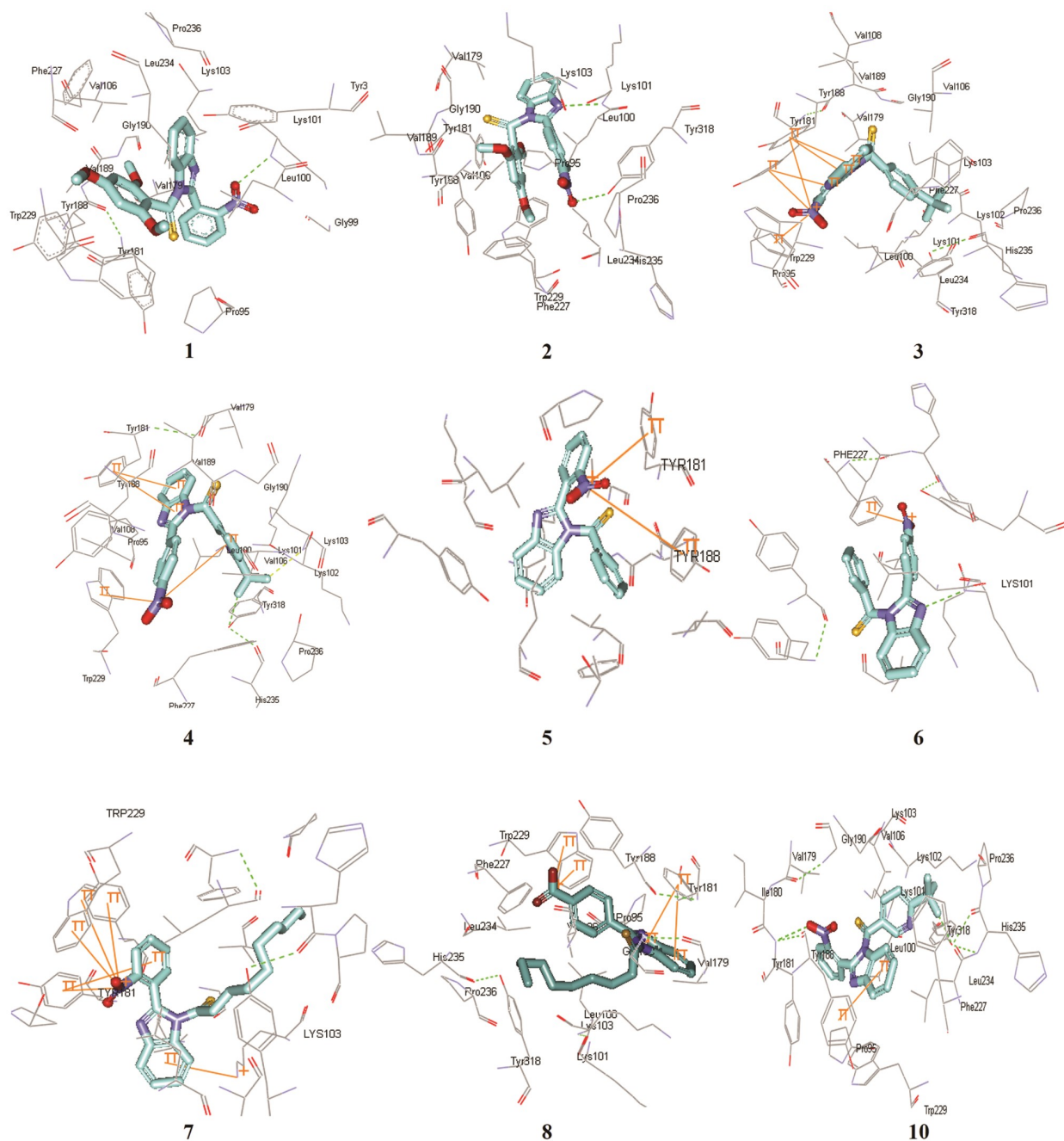


Figure 3 — Interaction of BPBIs with HIV-RT showing 'Butterfly' conformation

superimposed on complexes of HIV-1 RT and TIBO/nevirapine, the least RMSD was observed, showing the most favourable mode of interaction between BPBIs and HIV-1 RT. Compounds **21** and **22** did not dock, may be due to their larger size.

### Conclusion

We have exploited numerous benzimidazole derivatives to develop some potent and selective

inhibitors of HIV-1 RT by using an *in silico* structure-based approach. Docking results reveal that the designed BPBIs should have very good potency and some of the designed BPBIs may be more potent than the known inhibitors – nevirapine and TIBO. There is a good correlation between the predicted  $K_d$ , various energy terms and descriptors for all newly reported BPBIs against HIV-1 RT. Exploration of these relationships may be useful for prediction of the

activity of novel BPBIs. BPBI derivatives, like the other non nucleoside inhibitors, share a common butterfly like shape consisting of two wings: a benzimidazole moiety and a phenyl moiety (wing I and wing II, respectively). The third aromatic ring involving  $\pi$ - $\pi$  stacking and hydrophobic interactions significantly influences the interactions with HIV-1 RT. The ability of HIV-1 RT to accommodate the extra phenyl ring led us to examine additional aromatic substituents that might enhance the binding. Valuable information was obtained by the simulation results, which would be useful in designing new members of this class. Hydrogen bonds and van der Waals interactions played significant roles in the stabilisation of HIV-1 RT and BPBI complexes. Experimental and docking procedures for designing new BPBIs were focused on the variation of the substituents in the positions *N*-1 and *C*-2 of benzimidazole nucleus. Most of the BPBI inhibitors formed hydrogen bonds with the backbone nitrogen of Lys103 in the protein and contributed to drug potency, which can be helpful in designing of new ligands. Molecular modelling studies suggested that  $\pi$ -deficient aromatic ring of the benzothiamide system in **3**, **4**, **5**, **6**, **7**, **8**, **9**, **10** contributed to excellent binding properties of these compounds, probably through hydrophobic,  $\pi$ -stacking and charge transfer interactions. The 2/4-nitro phenyl benzimidazoles **4**, **9** and **16**, which showed the highest inhibitory activity against HIV-1 RT, represented a valuable advance in the search for novel NNRTIs and can be considered as a starting point for lead optimization, which is currently in progress.

#### Acknowledgement

The authors sincerely acknowledge the financial support from the Department of Biotechnology and Indian Council of Medical Research, Government of India.

#### References

- 1 Sarafianos S G, Marchand B, Das K, Himmel D M, Parniak M A, Hughes S H & Arnold E, *J Mol Biol*, 385 (2009) 693.
- 2 Singh R K, Yadav D, Rai D, Kumari G & Pannecoque C, *Eur J Med Chem*, 45 (2010) 3787.
- 3 Peng Z, Xuwang C, Dongyue L, Zengjun F, De Clercq E & Xinyong L, *Med Res Rev*, 33 (2013) 1.
- 4 Kumari, G & Singh R K, *Curr Pharm Des*, 19 (2013) 1767.
- 5 De Clercq E, *Biochem Pharmacol*, 84 (2012) 241.
- 6 Kumari G & Singh R K, *HIV&AIDS Review*, 11 (2012) 5.
- 7 De Clercq E, *Int J Antimicrob Agents*, 33 (2009) 307.
- 8 Mehellou Y & De Clercq E, *J Med Chem*, 53 (2010) 521.
- 9 De Clercq E, *Chem Biodiverse*, 1 (2004) 44.
- 10 Singh A, Yadav D, Yadav M, Dhamanage A, Kulkarni S & Singh R K, *Chem Biol Drug Des*, 85 (2015) 336.
- 11 Jonckheere H, Anne J & De Clercq E, *Med Res Rev*, 20 (2000) 129.
- 12 Singh A, Yadav M, Srivastava R, Singh N, Kaur R, Gupta S K & Singh R K, *Med Chem Res*, 25 (2016) 2842.
- 13 Tronchet J M & Seman M, *Curr Top Med Chem*, 3 (2003) 1496.
- 14 Lipinski C A, Lombardo F, Dominy B W & Feeney P J, *Adv Drug Deliv Rev*, 46 (2001) 3.
- 15 Ding J, Das K, Moereels H, Koymans L, Andries K, Janssen P A, Hughes S H & Arnold E, *Nature Struct Biol*, 2 (1995) 407.
- 16 Momany F A & Rone R, *J Comput Chem*, 13 (1992) 888.
- 17 Brooks B R, Bruccoleri R E, Olafson B D, States D J, Swaminathan S & Karplus M, *J Comput Chem*, 4 (1983) 187.
- 18 Venkatachalam C M, Jiang X, Oldfield T & Waldman F, *J Mol Graphics Modell*, 21 (2003) 289.
- 19 Mayo S L, Olafson B D & Goddard W A, *J Phys Chem*, 94 (1990) 8897.
- 20 Böhm H J, *J Comput Aided Mol Des*, 8 (1994) 623.
- 21 Böhm H J, *J Comput Aided Mol Des*, 12 (1998) 309.
- 22 Böhm H J, *J Comput Aided Mol Des*, 8 (1994) 243.
- 23 Wang R, Lu Y & Wang S, *J Med Chem*, 46 (2003) 2287.
- 24 Gehlhaar D K, Verkhivker G M, Rejto P A, Sherman C J, Fogel D B, Fogel L J & Freer S T, *Chem Biol*, 2 (1995) 317.
- 25 Muegge I & Martin Y C, *J Med Chem*, 42 (1999) 791.
- 26 Lagos C F, Caballero J, Gonzalez-Nilo F D, Mahana D P C & Perez-Acle T, *Chem Biol Drug Des*, 72 (2008) 360.
- 27 Gallivan J P & Dougherty D A, *Proc Natl Acad Sci (USA)*, 96 (1999) 9459.



